Supporting Information

Electroluminescence Efficiency of 30.3% for Yellow Thermally Activated Delayed Fluorescence Emitter with High Horizontal Emitting Dipole Ratio

Yan-Qing Tang,[1,†] Jing-Xiong Zhou,[1,†] Yan-Qing Li,[2,*] De-Zhi Yang,[3] Xin-Yi Zeng,[1] Kai Zhang,[4] Yi-Hui He,[1] Hao Ren,[1] Dong-Ge Ma,[3,*] Jian-Xin Tang[1,4,*]

[1] *Institute of Functional Nano & Soft Materials (FUNSOM), Jiangsu Key Laboratory for Carbon-Based Functional Materials & Devices, Soochow University, Suzhou 215123, China*, *E-mail: jxtang@suda.edu.cn (J.X. Tang)*

[2] *School of Physics and Electronic Science, Ministry of Education Nanophotonics and Advanced Instrument Engineering Research Center, East China Normal University, Shanghai 200062, China, E-mail: yqli@phy.ecnu.edu.cn (Y.Q. Li)*

[3] *Center for Aggregation-Induced Emission, Institute of Polymer Optoelectronic Materials and Devices, Guangdong Provincial Key Laboratory of Luminescence from Molecular Aggregates, State Key Laboratory of Luminescent Materials and Devices, South China University of Technology, Guangzhou 510640, People's Republic of China.*
E-mail: msdgma@scut.edu.cn (D.G. Ma)

[4] *Macao Institute of Materials Science and Engineering (MIMSE), Faculty of Innovation Engineering, Macau University of Science and Technology, Taipa 999078, Macao, China*

[†] These authors contributed equally to this work.

Experimental section

Synthesis of 3,6,12-tribromodibenzo[f,h]pyrido[2,3-b]quinoxaline (3,6,12-triBr-BPQ): A mixture of (3,6-dibromo-10-oxophenanthren-9(10H)-ylidene)oxonium (0.80 g, 2.18 mmol) and 5-bromopyridine-2,3-diamine (0.45 g, 2.40 mmol) was dissolved in 50 mL ethanol. The mixture solution was refluxed at 90 °C under N_2 atmosphere for 6 hours. The precipitate was collected by filtration and washed with sufficient ethanol to obtain the purified 3,6,12-triBr-BPQ without further purification (1.03 g, 1.99 mmol). The yield was 91 %.

Synthesis of 4,4',4''-(dibenzo[f,h]pyrido[2,3-b]quinoxaline-3,6,12-triyl)tris(N,N-diphenylaniline) (3,6,12-triTPA-BPQ): 3,6,12-triBr-BPQ (1.00 g, 1.93 mmol), (4 (diphenylamino)phenyl)boronic acid (1.84 g, 6.26 mmol), K_2CO_3 (0.79 g, 5.75 mmol) were added in a 60 mL mixture of 1,4-dioxane and water (10/1, v/v). Then, $Pd(PPh_3)_4$ (67 mg, 0.058 mmol) was added in a nitrogen atmosphere. After the solution was heated at 90 °C for 48 hours, the reaction mixture was cooled to room temperature. The product was poured into 100 mL of water, and then extracted with dichloromethane (DCM). The obtained layer was evaporated under reduced pressure and further purified via column chromatography using DCM as the eluent to afford an orange solid (1.53 g, 1.51 mmol). The yield was 77 %. ^{1}H NMR (400 MHz, $CDCl_3$) δ 9.54 (dd, J = 5.5, 2.9 Hz, 2H), 9.35 (d, J = 8.4 Hz, 1H), 8.75 (d, J = 2.4 Hz, 2H), 8.71 (d, J = 2.5 Hz, 1H), 7.96 (td, J = 8.4, 1.5 Hz, 2H), 7.73 (dd, J = 14.0, 8.5 Hz, 6H), 7.37 – 7.27 (m, 12H), 7.26 – 7.00 (m, 24H). ^{13}C NMR (101 MHz, $CDCl_3$) δ 153.22, 148.92, 148.08, 147.50, 147.16, 144.45, 144.08, 143.26, 143.09, 137.36, 136.96, 134.00, 133.35, 132.72, 129.53, 129.41, 129.14, 128.44, 128.23, 127.98, 127.11, 126.83, 126.67, 125.19, 124.76, 123.82, 123.53, 123.34, 123.00, 120.78, 120.57. MALDI-TOF-MS: m/z: calculated for $C_{70}H_{44}N_6$: 1010.41, found: 1011.550.

4,4',4''-(dibenzo[f,h]pyrido[2,3-b]quinoxaline-3,6,11-triyl)tris(N,N-diphenylaniline) (3,6,11-triTPA-BPQ): 3,6,11-triTPA-BPQ was prepared by the same procedure with 3,6,12-triTPA-BPQ excepting using the 6-bromopyridine-2,3-diamine (0.45 g, 2.40 mmol) instead of

5-bromopyridine-2,3-diamine. An orange solid of 2,7,12-triAC-BPQ (1.46 g, 1.39 mmol) were obtained by a two-step reaction. The yield was 70 %. ^{1}H NMR (400 MHz, $CDCl_3$) δ 9.57 – 9.35 (m, 1H), 9.18 (dd, J = 8.4, 2.8 Hz, 1H), 8.70 – 8.55 (m, 2H), 8.48 (d, J = 8.8 Hz, 1H), 8.16 (dd, J = 43.8, 8.8 Hz, 2H), 7.96 – 7.77 (m, 2H), 7.65 (ddd, J = 10.6, 8.7, 1.8 Hz, 4H), 7.41 – 7.26 (m, 12H), 7.24 – 7.00 (m, 24H). ^{13}C NMR (101 MHz, $CDCl_3$) δ 160.26, 150.23, 149.79, 148.86, 148.00, 147.95, 147.92, 147.52, 147.49, 147.15, 147.02, 144.99, 144.30, 143.91, 143.07, 142.97, 142.88, 142.45, 138.40, 137.24, 136.80, 136.64, 134.15, 134.09, 133.91, 132.69, 132.55, 132.24, 130.89, 129.53, 129.50, 129.39, 129.11, 128.53, 128.41, 128.23, 128.16, 126.81, 126.50, 125.43, 125.19, 124.75, 124.71, 123.97, 123.80, 123.58, 123.55, 123.48, 123.30, 123.25, 122.93, 122.41, 121.87, 120.61, 120.47. MALDI-TOF-MS: m/z: calculated for $C_{70}H_{44}N_6$: 1010.41, found: 1011.032.

Properties Characterization

Absorption and photoluminescence (PL) spectra were measured at room temperature with a PerkinElmer Lambda 750 UV-VIS spectrophotometer and a FM-4 fluorescence spectrophotometer (JY Company, France) at an excitation wavelength of 380 nm, respectively. Transient PL decay curves of the films were recorded by a Quantaurus-Tau transient spectrometer (C11367-32, Hamamatsu Photonics, Japan) with a pulse width of 100 ps and excitation wavelength of 373 nm under a vacuum condition. Low-temperature fluorescence and phosphorescence spectra were measured by LS 920 spectrometer (Einburgh company) at 77K. Φ_{PL} of the evaporation films was measured under nitrogen by absolute PL quantum yield measurement system (C9920-02G, Hamamatsu Photonics, Japan) using an integrating sphere. Cyclic voltammetry (CV) was performed on RST 3100 electrochemical work station. Thermal gravimetric analysis (TGA) was determined by HCT-2 instrument. Differential scanning calorimetry (DSC) analysis was performed with a Pyros diamond DSC thermal analyzer.

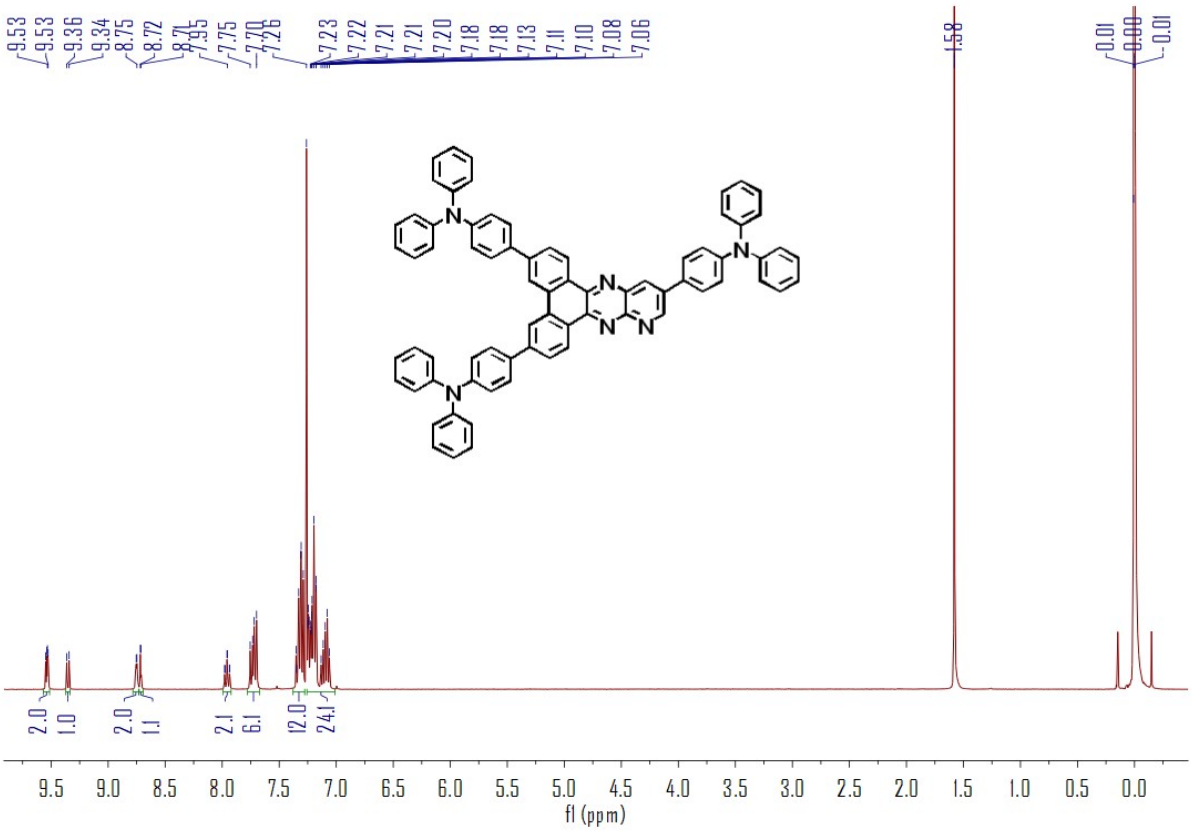

Figure S1. ^{1}H NMR spectrum of 3,6,12-triTPA-BPQ.

.

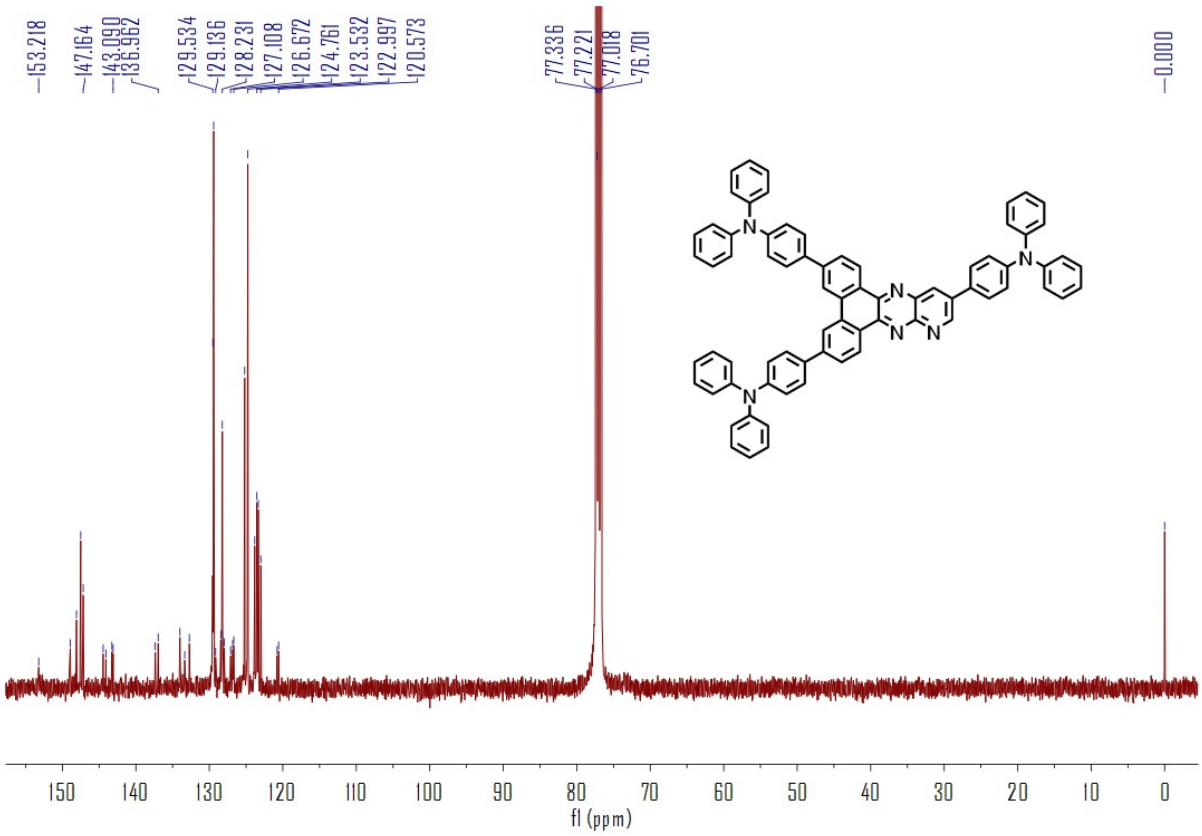

Figure S2. ^{13}C NMR spectrum of 3,6,12-triTPA-BPQ.

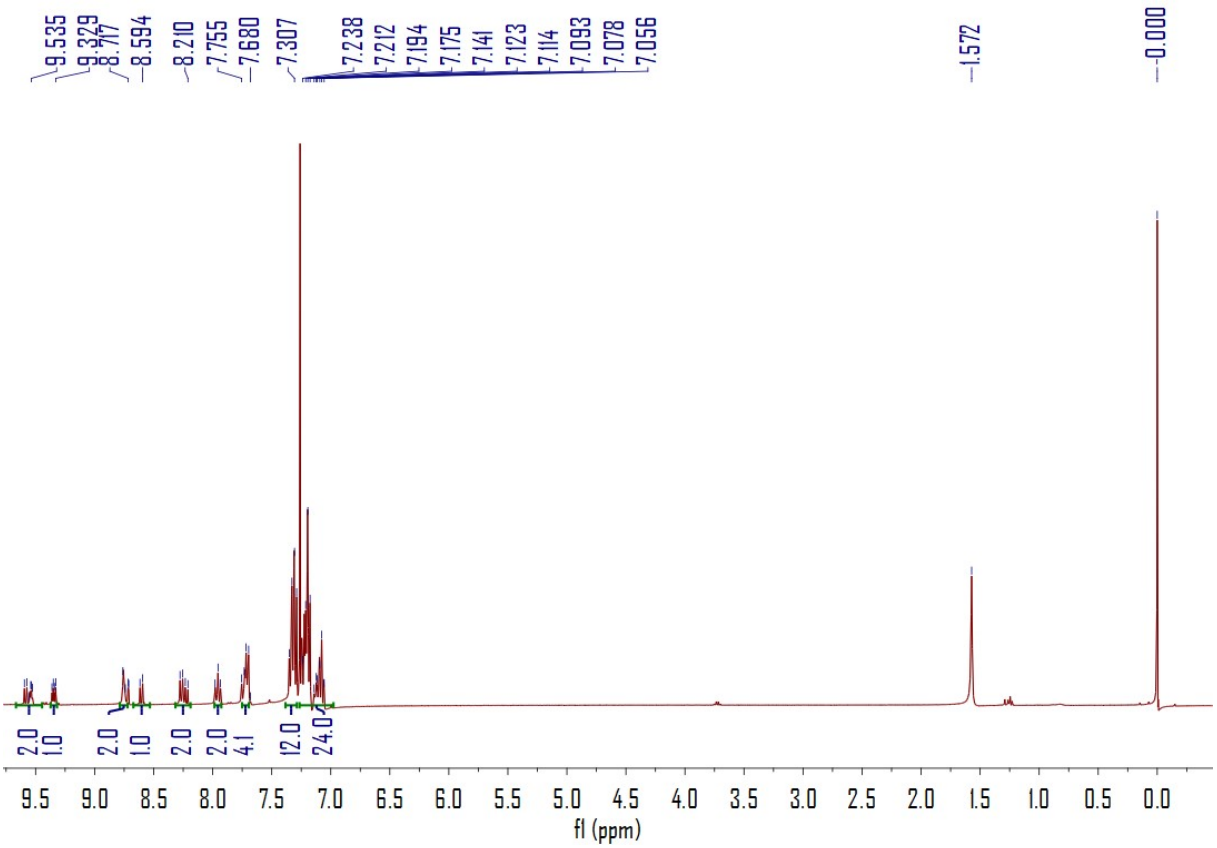

Figure S3. ^{1}H NMR spectrum of 3,6,11-triTPA-BPQ.

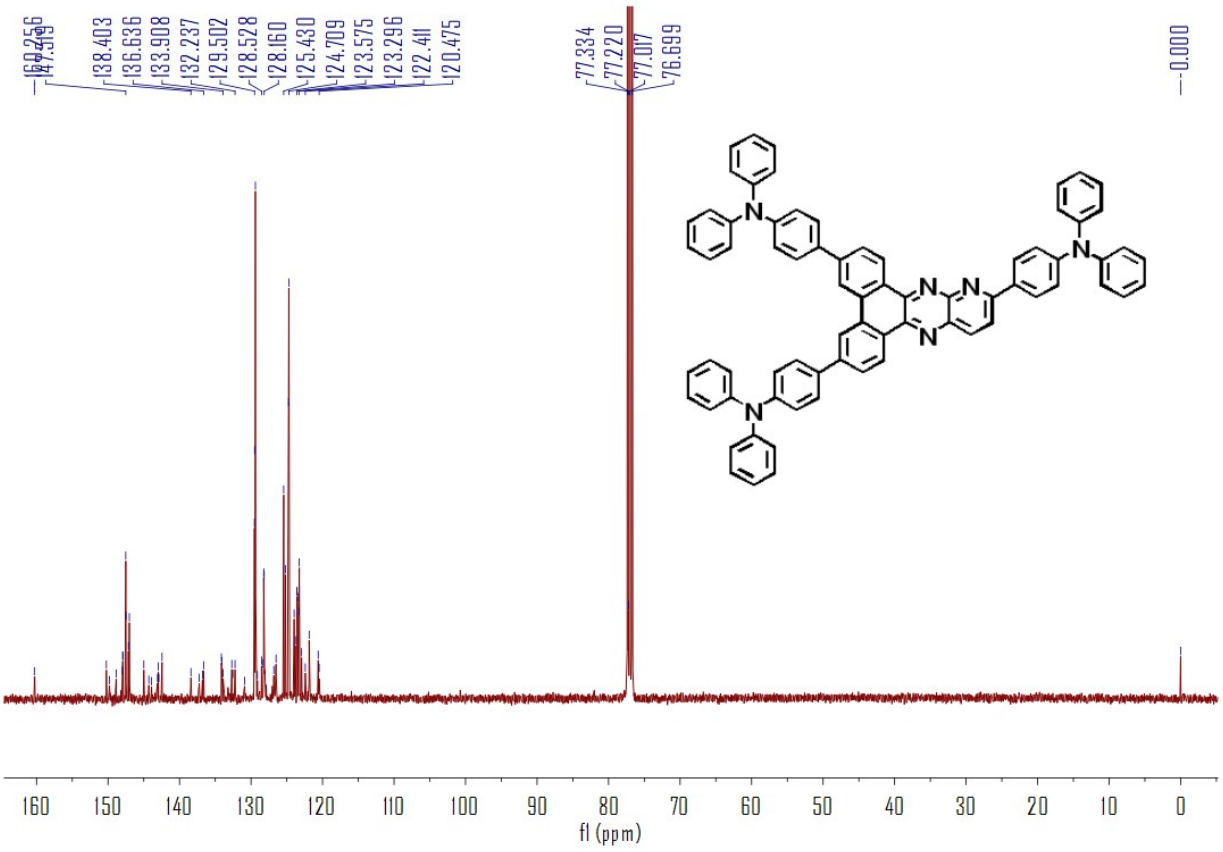

Figure S4. ^{13}C NMR spectrum of 3,6,11-triTPA-BPQ.

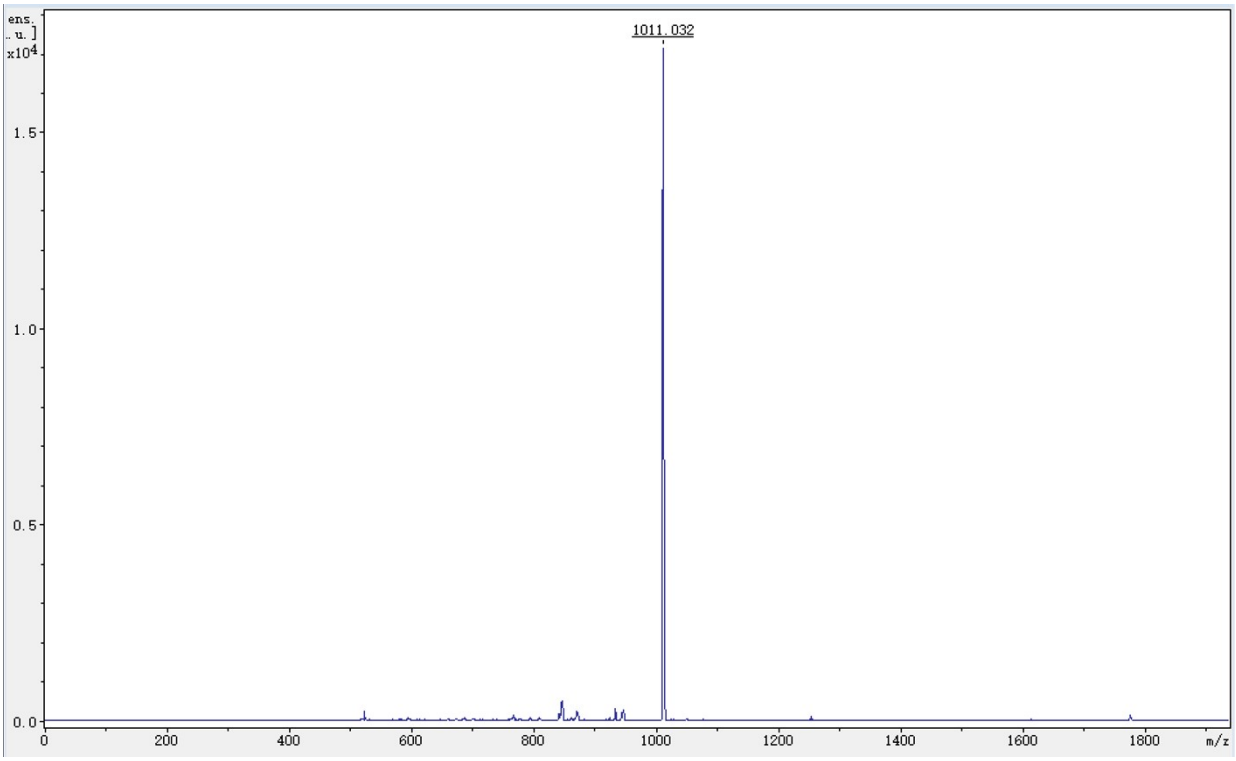

Figure S5. MALDI-TOF-MS of 3,6,11-triTPA-BPQ.

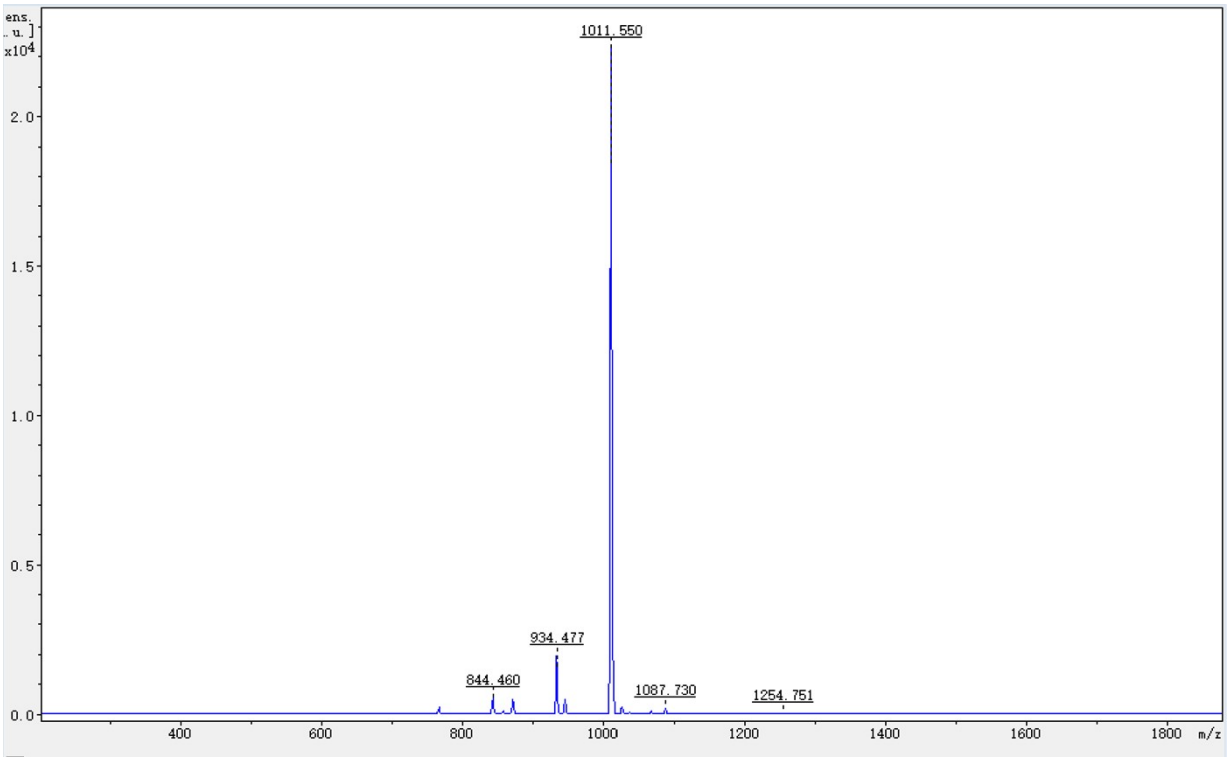

Figure S6. MALDI-TOF-MS of 3,6,12-triTPA-BPQ.

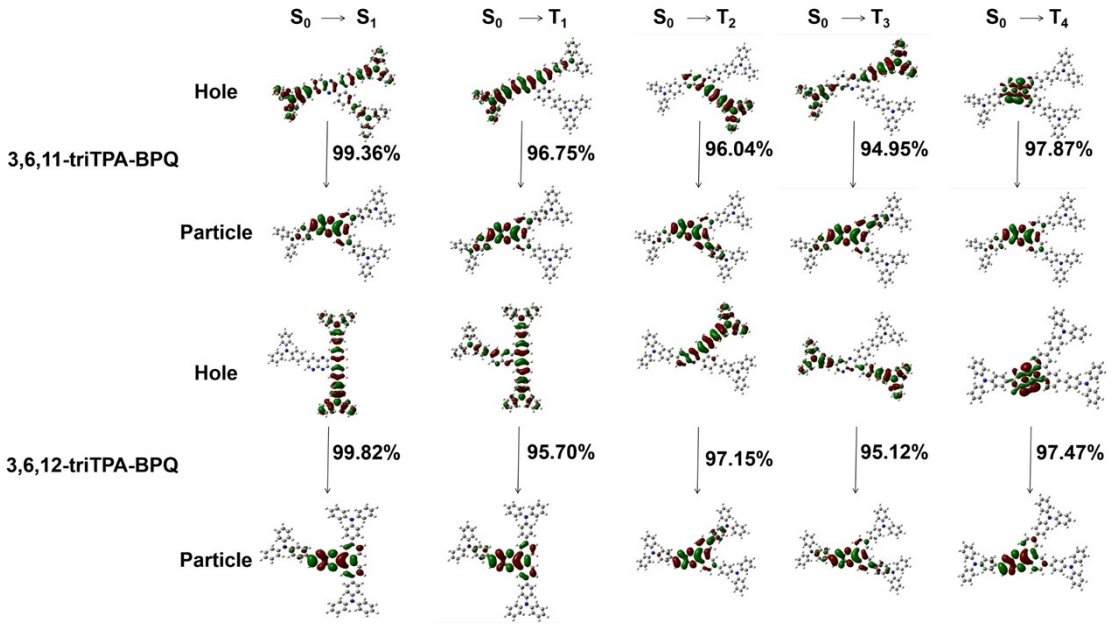

Figure S7. Natural transition orbital (NTO) analysis of 3,6,11-triTPA-BPQ and 3,6,12-triTPA-BPQ.

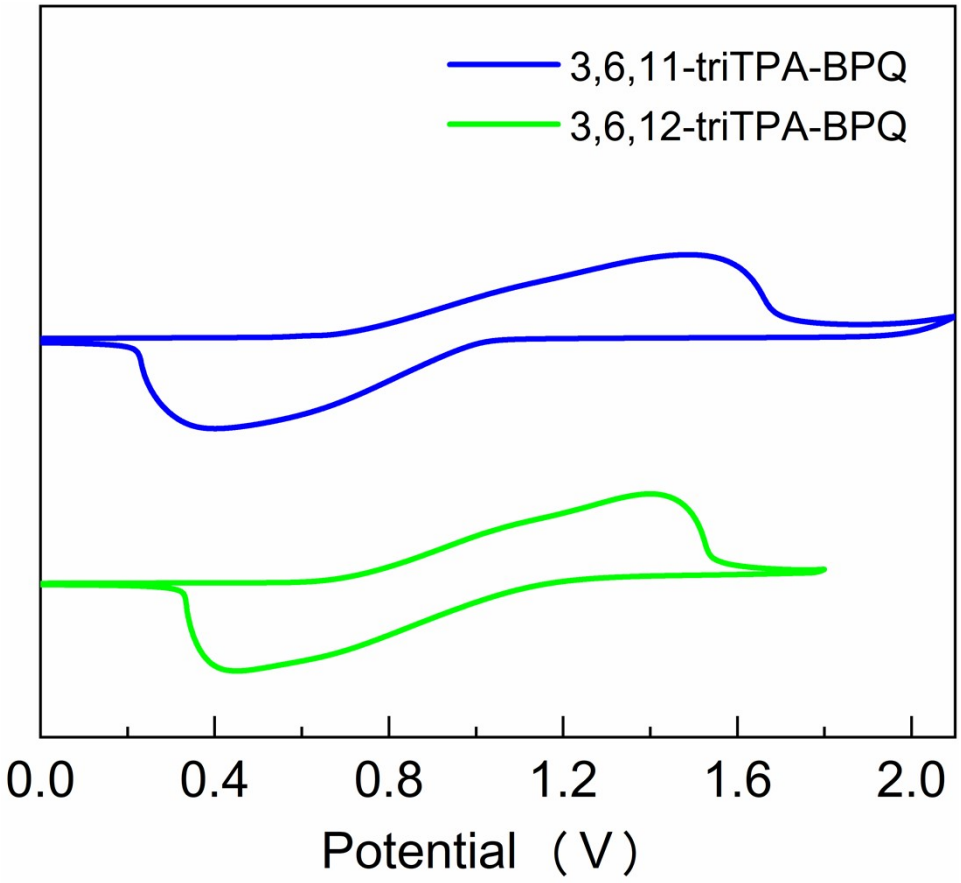

Figure S8. Cyclic voltammetry (CV) curves of 3,6,11-triTPA-BPQ and 3,6,12-triTPA-BPQ.

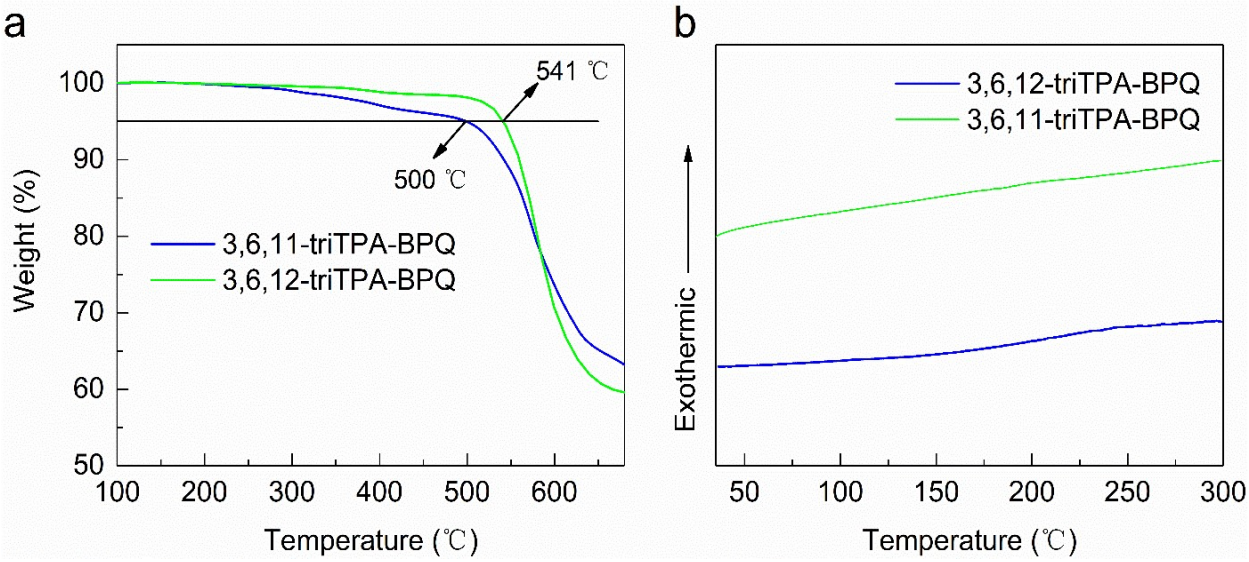

Figure S9. Thermal properties. a) Thermogravimetric analysis (TGA), and b) differential scanning calorimetry (DSC) curves of 3,6,11-triTPA-BPQ and 3,6,12-triTPA-BPQ.

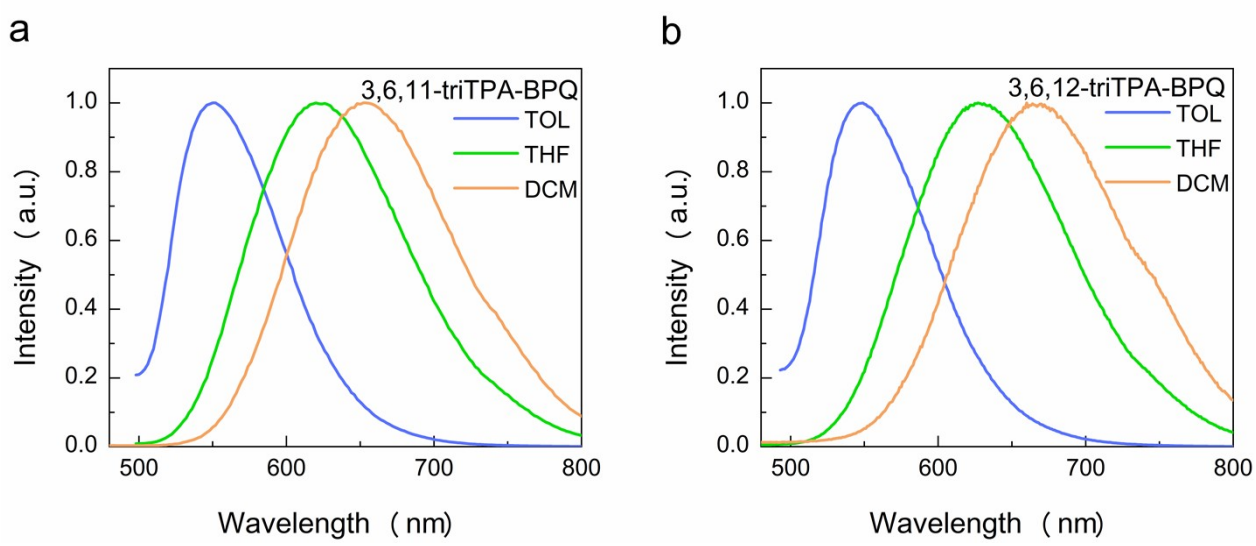

Figure S10. The emission spectra of a) 3,6,11-triTPA-BPQ and b) 3,6,12-triTPA-BPQ in toluene (TOL), tetrahydrofuran (THF), and dichloromethane (DCM).

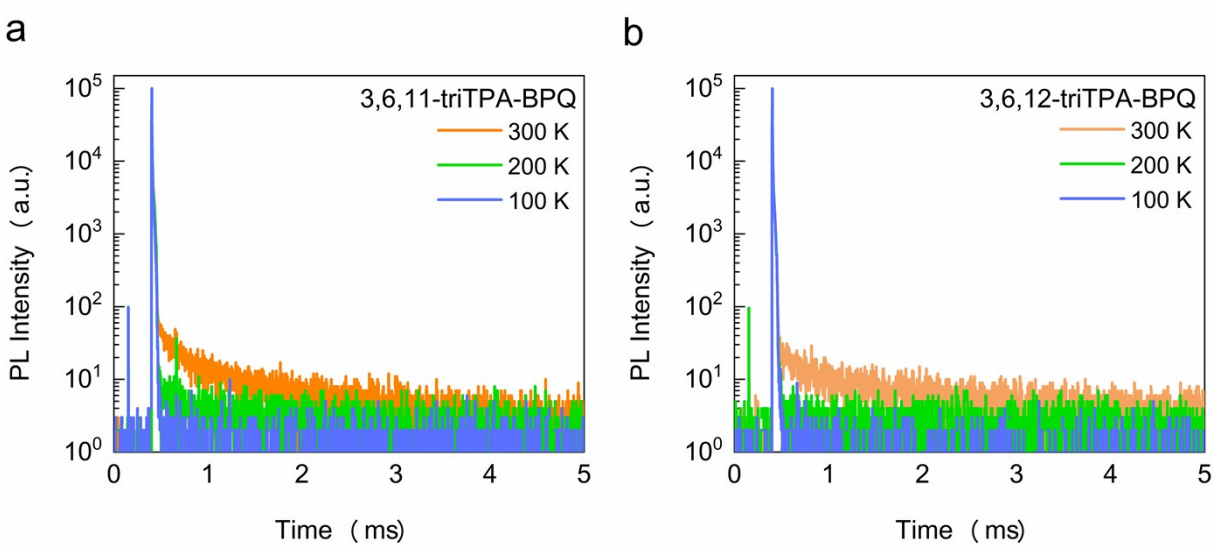

Figure S11. Temperature-dependent PL decay curves. a) 3,6,11-triTPA-BPQ:CBP film. b) 3,6,12-triTPA-BPQ:CBP film.

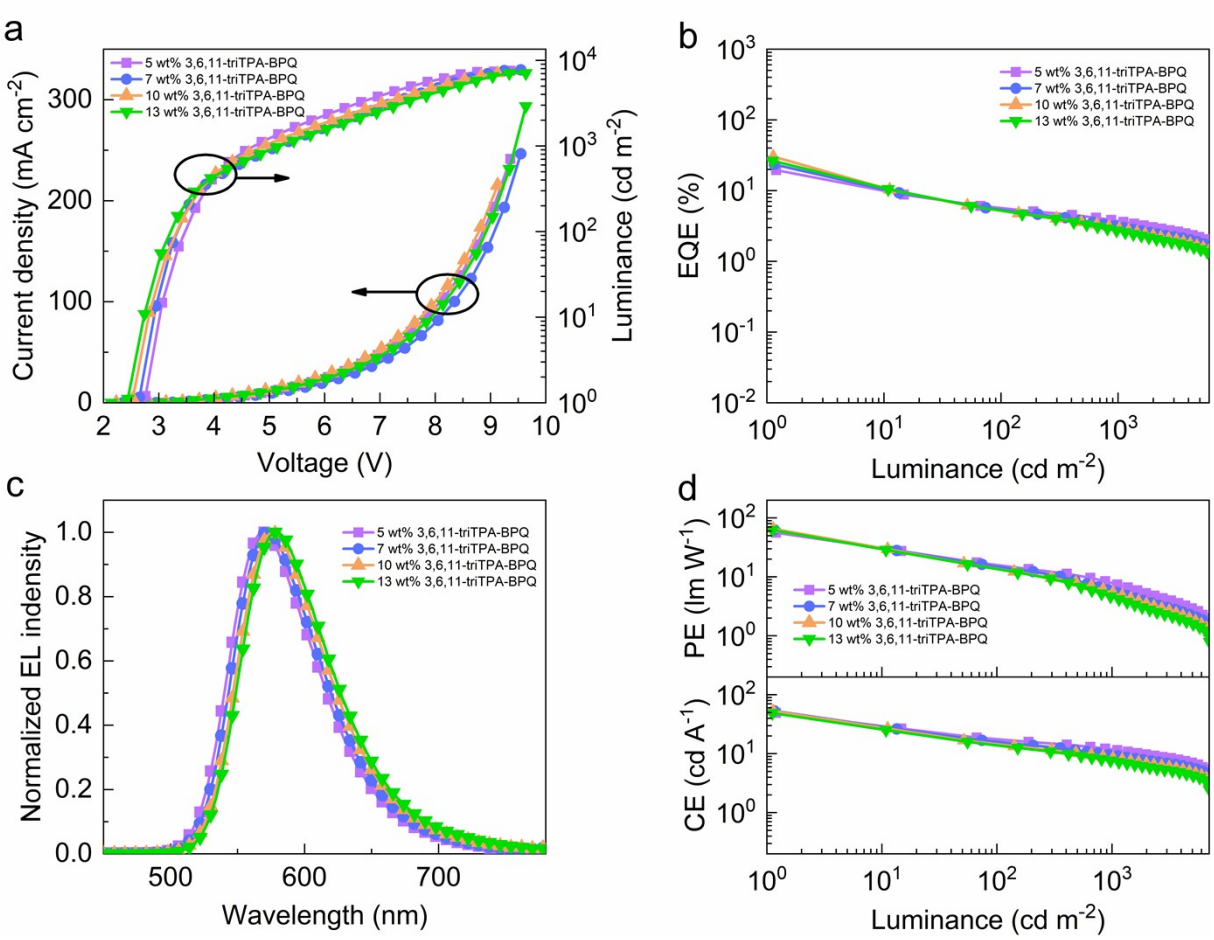

Figure S12. EL characteristics of yellow OLEDs based on different concentrations of 3,6,11-triTPA-BPQ. a) Current density-voltage-luminance (J-V-L) curves. b) EQE as a function of luminance. c) EL spectra. d) PE and CE versus luminance.

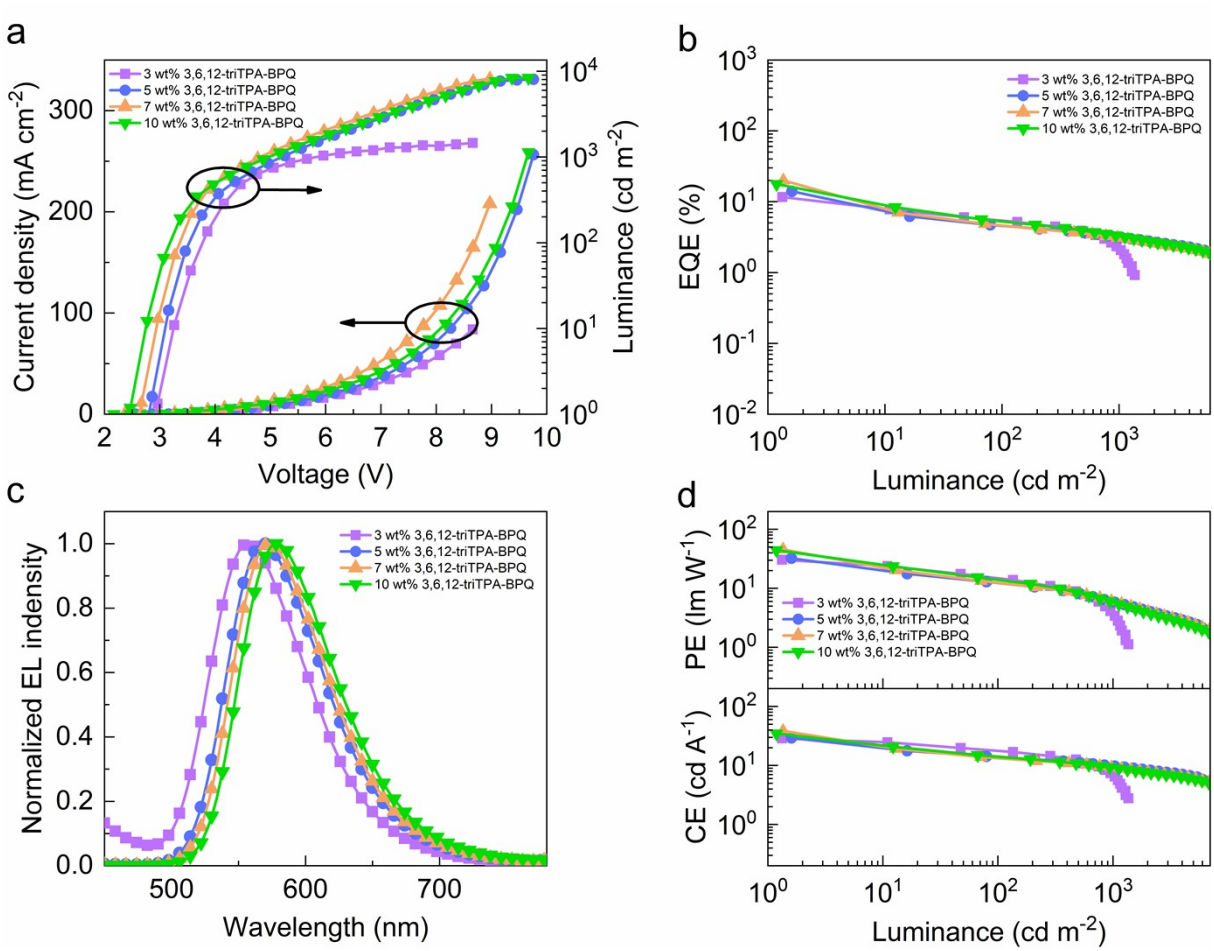

Figure S13. EL characteristics of yellow OLEDs based on different concentrations of 3,6,12-triTPA-BPQ. a) J-V-L curves. b) EQE versus luminance. c) EL spectra. d) PE and CE versus luminance.

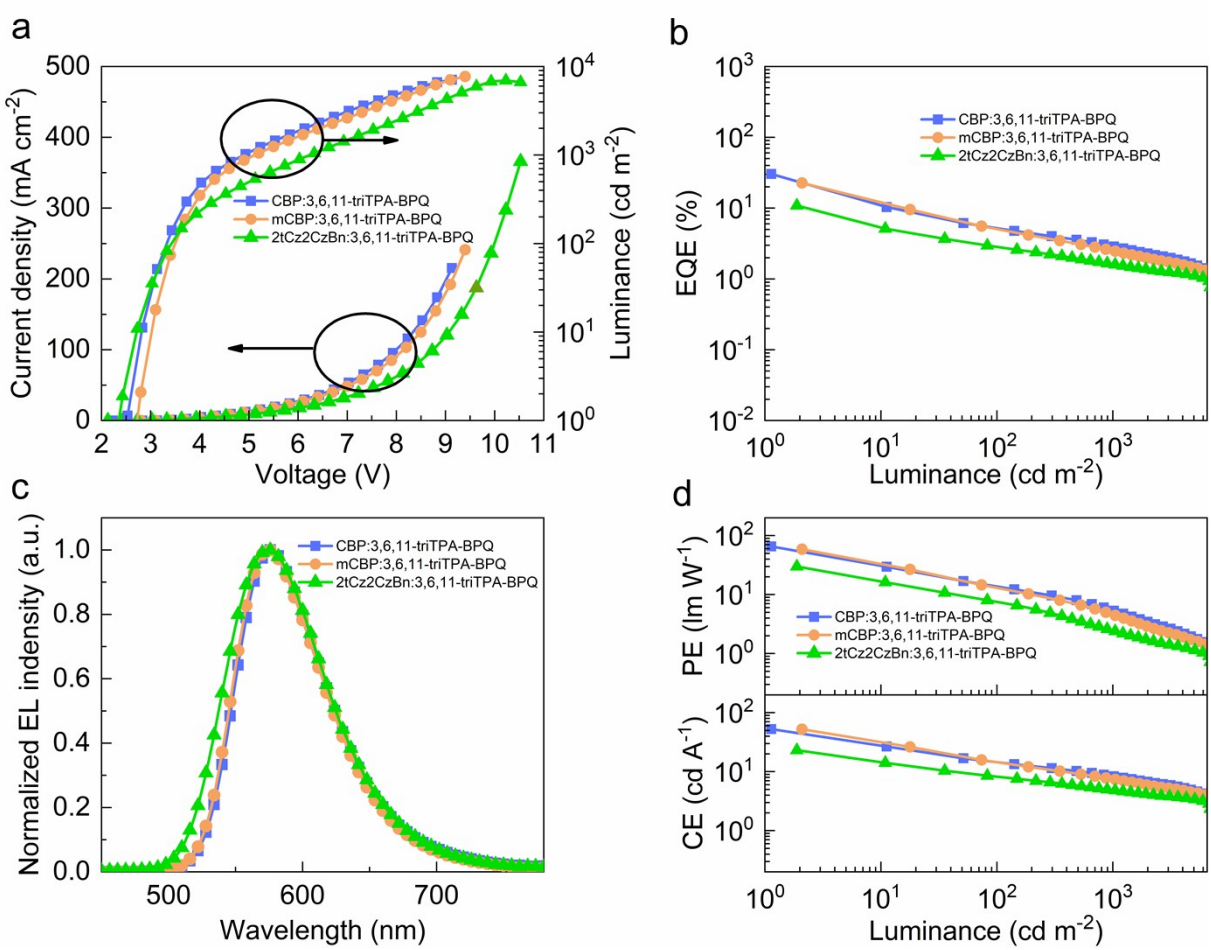

Figure S14. EL characteristics of yellow OLEDs based on varous host:10 wt% 3,6,11-triTPA-BPQ EML. a) J-V-L curves. b) EQE versus luminance. c) EL spectra. d) PE and CE versus luminance.

Table S1. Summary of theoretical calculation.

Emitters	HOMO [a] [eV]	LUMO [b] [eV]	S_1 [c] [eV]	T_1 [d] [eV]	ΔE_{ST} [eV]
3,6,11-triTPA-BPQ	-4.92	-2.31	2.29	1.97	0.32
3,6,12-triTPA-BPQ	-4.94	-2.33	2.32	2.03	0.29

[a] HOMO levels.

[b] LUMO levels.

[c] S_1 energy levels.

[d] T_1 energy levels.

Table S2. Photophysical data of doped in CBP films.

Doped films[a]	Φ_{PL} [%]	Φ_p [b] [%]	Φ_d [b] [%]	k_r [c] [10^5 s^{-1}]	k_{nr} [d] [10^4 s^{-1}]	k_{ISC} [e] [10^5 s^{-1}]	k_{RISC} [f] [10^3 s^{-1}]
3,6,11-triTPA-BPQ	94.0	35.1	58.9	2.13	1.28	3.94	3.86
3,6,12-triTPA-BPQ	78.7	31.6	47.1	1.88	4.00	4.06	3.05

a) Doped in CBP films.

b) Quantum yields for prompt (Φ_p) and delayed (Φ_d) component.

c) Radiative rates constants of S_1 ($k_r = \Phi_p/\tau_p$).

d) Nonradiative rates constants of S_1 ($k_{nr} = (1-\Phi_p)/\tau_p$).

e) Rate constants for ISC (S_1 to T_1), $k_{ISC} = k_p - k_F = k_p\,(1 - \Phi_p)$.

f) Rate constants for RISC (T_1 to S_1), $k_{RISC} = (k_p k_d)/(k_p - k_{ISC})$.

Table S3. EL performances of yellow TADF OLEDs based on 3,6,11-triTPA-BPQ emitter with different doping concentrations.

X [a] [wt %]	V_{on} [b] [V]	EQE [c] [%]	PE [c] [lm W^{-1}]	CE [c] [cd A^{-1}]	λ_{EL} [d] [nm]	CIE [d] [x, y]
5	2.8	19.4/5.1/3.6	55.9/13.6/7.4	49.1/15.9/11.5	570	(0.49, 0.51)
7	2.7	23.3/4.6/3.0	63.0/12.3/5.4	53.2/13.9/9.1	572	(0.50, 0.50)
10	2.5	30.3/4.8/2.9	65.4/12.2/5.3	52.7/13.4/8.4	576	(0.51, 0.48)
13	2.4	26.4/4.7/2.6	62.7/11.8/4.2	48.7/12.6/7.2	578	(0.52, 0.47)

[a)] Doping concentration of 3,6,11-triTPA-BPQ emitter.

[b)] Turn-on voltage at a brightness is 1 cd m^{-2}.

[c)] The maximum EQE, PE, and CE values at 1/100/1000 cd m^{-2}.

[d)] The wavelength of the EL peak and CIE 1931 coordinate at a brightness of 1000 cd m^{-2}.

Table S4. EL performances of yellow TADF OLEDs based on 3,6,12-triTPA-BPQ emitter with different doping concentrations.

X [a] [wt %]	V_{on} [b] [V]	EQE [c] [%]	PE [c] [lm W^{-1}]	CE [c] [cd A^{-1}]	λ_{EL} [d] [nm]	CIE [d] [x, y]
3	3.0	11.6/5.2/2.1	30.5/13.8/3.4	28.8/17.0/6.5	556	(0.41, 0.49)
5	2.9	14.0/4.1/3.1	32.2/10.6/5.8	29.3/12.7/9.7	568	(0.48, 0.51)
7	2.7	19.9/4.1/3.0	45.4/10.5/5.5	38.6/11.9/8.9	574	(0.50, 0.49)
10	2.5	17.7/4.7/3.2	44.3/11.9/5.4	34.8/12.7/8.9	578	(0.52, 0.48)

[a)] Doping concentration of 3,6,12-triTPA-BPQ emitter.

[b)] Turn-on voltage at a brightness is 1 cd m^{-2}.

[c)] The maximum EQE, PE, and CE values at 1/100/1000 cd m^{-2}.

[d)] The wavelength of the EL peak and CIE 1931 coordinate at a brightness of 1000 cd m^{-2}.

Table S5. EL performances of yellow TADF OLEDs based on 3,6,11-triTPA-BPQ emitter.

EMLs	V_{on} [a] [V]	EQE [b] [%]	PE [b] [lm W^{-1}]	CE [b] [cd A^{-1}]	λ_{EL} [c] [nm]	CIE [c] [x, y]
CBP:3,6,11-triTPA-BPQ	2.5	30.3	65.4	52.7	576	(0.51, 0.48)
mCBP:3,6,11-triTPA-BPQ	2.7	22.6	58.6	52.2	574	(0.51, 0.49)
2tCz2CzBn:3,6,11-triTPA-BPQ	2.4	10.9	29.9	23.1	574	(0.49, 0.50)

[a] Turn-on voltage at a brightness is 1 cd m^{-2}.

[b] The maximum EQE, PE, and CE values.

[c] The wavelength of the EL peak and CIE 1931 coordinate at a brightness of 1000 cd m^{-2}.

Table S6. Summary of PLQY based on 3,6,11-triTPA-BPQ and 3,6,12-triTPA-BPQ doped CBP films.

Emitters	X [a] [wt %]	PLQY [b] [%]
3,6,11-triTPA-BPQ	5/7/10/13	82.9/86.9/94.0/74.1
3,6,12-triTPA-BPQ	3/5/7/10	32.3/59.4/78.4/56.5

[a)] Doping concentration of 3,6,11-triTPA-BPQ and 3,6,12-triTPA-BPQ emitter.

b) PLQY of the doped film (20 nm) at the corresponding concentration.

Table S7. Summary of SOC (ξ) and energy gap values ($T_n \rightarrow S_1$) of 3,6,11-triTPA-BPQ.

Tn [n≥1]	Tn [eV]	energy gap(ΔE_{S1Tn}) [eV][a]	ξ [cm^{-1}]
T_1	1.97	0.32	0.05
T_2	2.19	0.10	0.04
T_3	2.28	0.01	0.09
T_4	2.56	-0.27	0.25
T_5	2.60	-0.31	0.07

a) energy gap between T_n and S_1, a negative value indicates that the T_n state is higher than the S_1 state.

Table S8. Summary of SOC(ξ) and energy gap values ($T_n \rightarrow S_1$) of 3,6,12-triTPA-BPQ.

Tn [n≥1]	Tn [eV]	energy gap(ΔE_{S1Tn}) [eV][a]	ξ [cm^{-1}]
T_1	2.03	0.29	0.052
T_2	2.18	0.14	0.041
T_3	2.29	0.03	0.088
T_4	2.56	-0.24	0.252
T_5	2.62	-0.30	0.066

[a] energy gap between T_n and S_1, a negative value indicates that the T_n state is higher than the S_1 state.